

## Time-dependent nanoscale plasticity in nanocrystalline nickel rods and tubes

Jung-A Lee<sup>a</sup>, Brandon B. Seo<sup>b</sup>, In-Chul Choi<sup>a</sup>, Moo-Young Seok<sup>a</sup>, Yakai Zhao<sup>a</sup>, Zeinab Jahed<sup>b</sup>, Upadrasta Ramamurty<sup>c,d</sup>, Ting Y. Tsui<sup>b,e,\*</sup>, Jae-il Jang<sup>a,\*\*</sup>

<sup>a</sup> Division of Materials Science and Engineering, Hanyang University, Seoul 133-791, South Korea

<sup>b</sup> Department of Mechanical Engineering, University of Waterloo, Waterloo, ON N2L 3G1, Canada

<sup>c</sup> Department of Materials Engineering, Indian Institute of Science, Bangalore 560012, India

<sup>d</sup> Center of Excellence for Advanced Materials Research, King Abdulaziz University, Jeddah 21589, Saudi Arabia

<sup>e</sup> Waterloo Institute of Technology, University of Waterloo, Waterloo, ON N2L 3G1, Canada

### ARTICLE INFO

#### Article history:

Received 7 August 2015

Received in revised form 8 September 2015

Accepted 8 September 2015

Available online 20 September 2015

#### Keywords:

Nanocrystalline Ni

Time-dependent plasticity

Microcompression

Creep

Strain-rate sensitivity

### ABSTRACT

Time-dependent nanoscale plasticity of nanocrystalline nickel at room temperature was critically explored through a series of micropillar creep and quasi-static compression experiments on rod and tube specimens fabricated by electron beam lithography and electroplating. Enhanced creep rates in tubes as compared to rods, establishes the facilitating role played by the free surface in time-dependent deformation. Creep stress exponent,  $n$ , and strain-rate sensitivity,  $m$ , were compared to examine connections between creep and the rate-dependent plasticity, if any.

© 2015 Elsevier Ltd. All rights reserved.

Plastic deformation in nanocrystalline (nc) metals and alloys (with a grain size  $d < 100$  nm) is a topic of current and active research, with most recent focus on the mechanical behavior of small-scale nc samples through micro-/nano-pillar testing [1–11], especially of metals with face-centered cubic crystal structure (Ni [2–7], Cu [8,9], Pt [10], and Rh [11]). In these studies, the effects of sample size on the yield strength and flow stress were explored [3–5,9,10]. Results of one study [3] indicate that “smaller is stronger” which is similar to that typically observed in the pillars of single crystal or coarse-grained metals [12–14]. A number of other studies (e.g., for the pillars of Ni–W ( $d \sim 60$  nm) [4], Ni ( $d \sim 12$  nm) [5], Cu ( $d \sim 100$  nm) [9], and Pt ( $d \sim 12$  nm) [10]) suggest an opposite trend, i.e., “smaller is weaker.” Although the mechanism for this size-dependent weakening of the nc pillars has not been understood in detail yet, it was thought to be related to the role of free surfaces. For instance, Jang and Greer [4] postulated that a free surface can enhance grain boundary (GB)-mediated deformation process in Ni–W pillars structures.

Recently, the time-dependent plasticity at room temperature (RT) of nc pillars was also researched [6,7]. Choi et al. [6] observed creep

deformation at RT of a series of nc Ni pillars having different pillar diameter  $D$  and revealed that the creep gets more pronounced as  $D$  gets smaller, and suggested that the increased surface-to-volume ratio (SVR) with decreasing  $D$  is possibly the reason behind this observation. However, the precise connection between change in SVR and sample size effect requires critical investigation, as simply changing the deforming volume (irrespective of the roles of surfaces) can also bring about other changes in metallurgical and mechanical environments. One such example is that when the sample volume is changed, the size and distribution of defects that affect the mechanical behavior also change. To address this, which is the first motive of this study, we employ nc pillars with the same outer  $D$  but with substantially different SVR and perform creep experiments. The second objective of this study is to establish a quantitative relation between creep and rate-dependency of flow stress in terms of the material parameter that governs each of these phenomena; i.e., the stress exponent  $n(= \frac{\partial \ln \dot{\epsilon}}{\partial \ln \sigma} \sigma, T)$  for creep and strain-rate sensitivity  $m(= \frac{\partial \ln \sigma}{\partial \ln \dot{\epsilon}} \epsilon, T)$  for rate-dependency of flow stress. Due to the similarity in the mathematical description of these material constants,  $n$  is often estimated from  $m$  (which is obtained from the quasi-static uniaxial tests conducted at various strain rates) or vice versa, by simple conversion, viz.  $n = 1/m$  [15–18]. Nevertheless, the appropriateness of this conversion for nc pillars has not been systematically examined yet. This may be due to the difficulties in conducting meaningful constant strain-rate pillar compression tests in

\* Corresponding author at: Department of Mechanical Engineering, University of Waterloo, Waterloo, ON N2L 3G1, Canada.

\*\* Corresponding author at: Division of Materials Science and Engineering, Hanyang University, Seoul 133-791, South Korea.

E-mail addresses: [tttsui@uwaterloo.ca](mailto:tttsui@uwaterloo.ca) (T.Y. Tsui), [jjjang@hanyang.ac.kr](mailto:jjjang@hanyang.ac.kr) (J-i. Jang).

large numbers, because the pillars are often prepared by focused ion beam (FIB) milling that requires much time and cost.

To address the above issues, here we performed a series of creep and constant strain-rate tests, both in uniaxial compression, on nc Ni pillars prepared through electroplating processes. There are three clear advantages in utilizing such pillars. First, it was possible to prepare pillars having different SVRs but the same outer  $D$ , such as rods and tubes with the same outer  $D$ . Second, we could produce several hundreds of pillars in single batch of process, which made it possible to conduct statistically significant large number of constant strain-rate tests. Third, we could avoid any possible surface effect induced during FIB milling process and thus related artifacts [19]. It is also noteworthy that pillar compression creep test is known to overcome the issues arising from nanoindentation creep test [20].

Two types of nc Ni pillars (including rods and tubes) were fabricated via electron beam lithography and electroplating process [19]. Silicon substrates covered with thin Ti ( $\sim 20$  nm) and Au ( $\sim 20$ – $60$  nm) seed layers were spin coated with polymethylmethacrylate (PMMA) resist. Arrays of circular and ring-shaped via-holes were patterned in the PMMA using electron beam lithography. Subsequently, patterned PMMA molds were filled with nc Ni by electroplating. For electroplating, a commercial grade pure Ni was used as anode and the solution was made of Ni (II) sulfate hexahydrate (99%, Sigma Aldrich), Ni (II) chloride (98%, Sigma Aldrich), boric acid (BX0865, EMD Millipore), and organic additive saccharin (98%, Sigma Aldrich). After electroplating, the remaining PMMA resist was removed with acetone. A specific advantage of this technique is that strong sample uniformity across each substrate can be obtained through this FIB-less fabrication of pillars. Representative microstructure of the pillars was examined using transmission electron microscopy (TEM), JEM-2010F (JEOL Ltd., Tokyo, Japan).

Both quasi-static, constant strain-rate compression tests and constant-load creep tests of the pillars were performed at RT using Nanoindenter XP (formerly MTS; now Keysight Tech., Oak Ridge, TN) with a FIB-milled cylindrical diamond punch having a top diameter of  $\sim 14$   $\mu\text{m}$ . During the creep tests under compressive loading, the load was increased up to the desired maximum stress level (i.e., 600, 800, 1000 MPa, respectively), then held for 1000 s, and finally removed at the same rate as the loading segment. During the quasi-static compression tests, the rods and tubes were loaded under strain rates ( $\dot{\epsilon}$ ) ranging from 0.0001 to 0.005/s. Pillar morphologies were imaged before and after the nanomechanical testing using scanning electron microscopy (SEM), JSM-6330F (JEOL Ltd., Tokyo, Japan). Additionally, in-situ compression tests were performed on rods inside a Quanta 250 FEG SEM (FEI Inc., Hillsboro, OR) using a PI 85 picoindenter (Hysitron Inc., Minneapolis, MN) at relatively high  $\dot{\epsilon}$  (0.002–0.01/s).

Fig. 1 exhibits representative SEM and TEM images showing the shapes and microstructures of as-fabricated pillars. The SEM

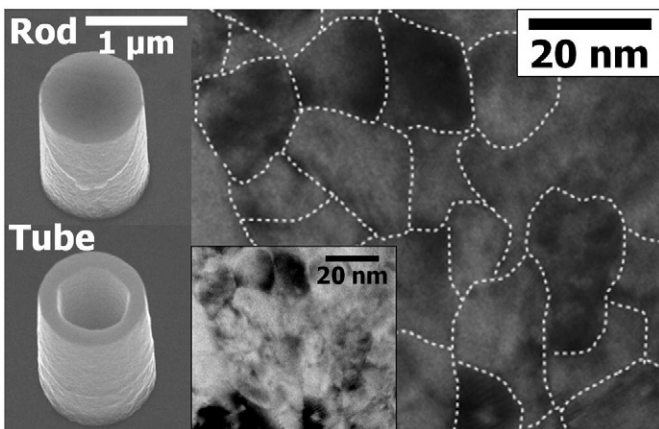


Fig. 1. Representative SEM and TEM images (with inset TEM image without dashed line) showing the geometry and grain structure of as-fabricated nc Ni pillars.

micrographs reveal that pillar tops are flat and there is almost no taper between sidewalls and substrates. Nominal outer  $D$  and aspect ratio of both rods and tubes are  $\sim 1000$  nm and  $\sim 1.7$ , respectively, and sidewall thickness of the tubes is  $\sim 175$  nm. As shown in the high-resolution TEM image in Fig. 1, the average grain size  $d$  of rods was determined as  $\sim 12$  nm. Although TEM observation of tubes was not performed here, similar microstructure was expected for tubes since tubes and rods were prepared on the same substrate and in the same solution [5].

First, constant-load compressive creep tests were conducted on rods and tubes. From the load–displacement ( $P$ – $h$ ) curves recorded during the tests, engineering stress  $P/A_0$  (where  $A_0$  is the initial cross-sectional area of pillar) vs. engineering strain  $h/L_0$  (where  $L_0$  is the initial pillar height) plots was obtained, as shown in Fig. 2a. The level of the applied stress for the load-holding sequence (i.e., creep stress  $\sigma_{\text{creep}}$ ) is within nominal elastic range, which manifests as superimposition of the loading portion in stress–strain curves. For both rods and tubes, the maximum value of creep strain generated during the hold segment ( $\epsilon_{\text{creep}}$ ) increases obviously with  $\sigma_{\text{creep}}$ . This stress-dependency of the maximum  $\epsilon_{\text{creep}}$  supports that the observed creep behavior is not an artifact caused by thermal drift which cannot depend on the level of applied load (and thus  $\sigma_{\text{creep}}$ ) [21]. Variation of  $\epsilon_{\text{creep}}$  with the hold time ( $t_{\text{hold}}$ ) curves (for  $\sigma_{\text{creep}} = 1000$  MPa) is provided in the inset of Fig. 2b. These creep curves apparently consist of two regimes in the early stages: primary (transient) creep regime and secondary creep regime where the apparent  $\epsilon_{\text{creep}}$  vs.  $t_{\text{holding}}$  relation shows a higher linearity. This two-regime behavior also supports that the creep observed in this study is not caused by thermal drift, because thermal drift is not expected to induce this two-regime curves [6]. As shown in the figure, at a given  $\sigma_{\text{creep}}$ ,  $\epsilon_{\text{creep}}$  obtained on tubes was always higher

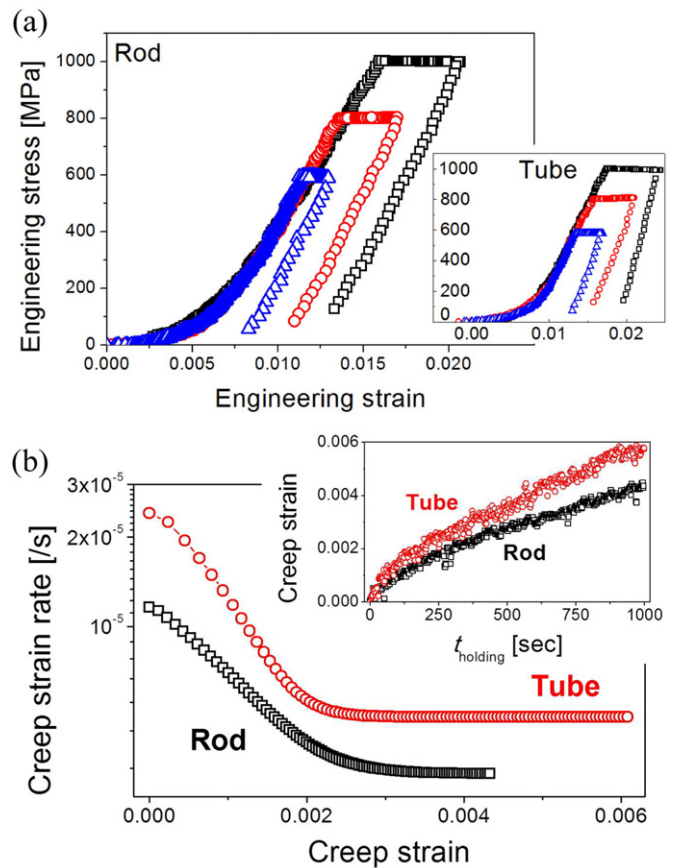


Fig. 2. Results of creep tests: (a) Representative stress–strain curves from creep tests; (b) example (for  $\sigma_{\text{creep}} = 1$  GPa) of the logarithmic creep strain rate vs. creep strain relation (with inset plot of creep strain vs. holding time).

Download English Version:

<https://daneshyari.com/en/article/7912506>

Download Persian Version:

<https://daneshyari.com/article/7912506>

[Daneshyari.com](https://daneshyari.com)